




Article

Antiviral Effect of pIFNLs against PEDV and VSV Infection in Different Cells

Jing Chen ^{1,2}, Wang Xu ², Peiheng Li ², Lina Song ², Yuhang Jiang ², Pengfei Hao ², Zihan Gao ², Wancheng Zou ², Ningyi Jin ^{1,2,*} and Chang Li ^{2,*} 

¹ Key Laboratory for Zoonosis Research, Ministry of Education, College of Veterinary Medicine, Jilin University, Changchun 130062, China

² Research Unit of Key Technologies for Prevention and Control of Virus Zoonoses, Chinese Academy of Medical Sciences, Changchun Veterinary Research Institute, Chinese Academy of Agricultural Sciences, Changchun 130122, China

* Correspondence: ningyik@126.com (N.J.); lichang78@163.com (C.L.)

Abstract: Type III and type I interferon have similar mechanisms of action, and their different receptors lead to different distributions in tissue. On mucosal surfaces, type III interferon exhibits strong antiviral activity. Porcine epidemic diarrhea virus (PEDV) is an economically important enteropathogenic coronavirus, which can cause a high incidence rate and mortality in *piglets*. Here, we demonstrate that porcine interferon lambda 1 (pIFNL1) and porcine interferon lambda 3 (pIFNL3) can inhibit the proliferation of vesicular stomatitis virus with an enhanced green fluorescent protein (VSV-EGFP) in different cells, and also show strong antiviral activity when PEDV infects Vero cells. Both forms of pIFNLs were shown to be better than porcine interferon alpha (pIFN α), the antiviral activity of pIFNL1 is lower than that of pIFNL3. Therefore, our results provide experimental evidence for the inhibition of PEDV infection by pIFNLs, which may provide a promising treatment for the prevention and treatment of Porcine epidemic diarrhea (PED) in *piglets*.

Keywords: pIFNLs; pIFN α ; VSV-EGFP; PEDV; antiviral activity



Citation: Chen, J.; Xu, W.; Li, P.; Song, L.; Jiang, Y.; Hao, P.; Gao, Z.; Zou, W.; Jin, N.; Li, C. Antiviral Effect of pIFNLs against PEDV and VSV Infection in Different Cells. *Int. J. Mol. Sci.* **2022**, *23*, 9661. <https://doi.org/10.3390/ijms23179661>

Academic Editor: James K. Bashkin

Received: 12 July 2022

Accepted: 20 August 2022

Published: 26 August 2022

Publisher's Note: MDPI stays neutral with regard to jurisdictional claims in published maps and institutional affiliations.



Copyright: © 2022 by the authors. Licensee MDPI, Basel, Switzerland. This article is an open access article distributed under the terms and conditions of the Creative Commons Attribution (CC BY) license (<https://creativecommons.org/licenses/by/4.0/>).

1. Introduction

The first interferon (IFN) described in modern medical research was type I IFN. Interferon plays an important role in the innate immune systems of vertebrates and has gained much attention in modern medical research [1]. The biological functions include the modulation of innate and adaptive immune responses, anti-proliferative effects, and most importantly, antiviral properties [2,3].

The type III IFNs or IFNLs were described along with type I IFNs [4,5]. IFNLR1 and IL-10R2 are heterodimeric receptors that are used by type III IFNs to signal, whereas IL-28R1 is used by type I IFNs [6–8]. The expression of IFNLR1 is not ubiquitous but appears to be limited to epithelial cells and certain immune cells [9–13]. Throughout history, the limited tropism of the type III IFN receptor has led to the hypothesis that type III IFNs exhibit unique properties on mucosal surfaces [13–20].

While type I and type III IFNs differ from sequence and structural perspectives, as well as using two different receptor complexes, cytokines induce a remarkably similar panel of interferon-stimulated genes (ISGs) in response to interferons. In the first instance, the binding of type I and III IFNs to IFN receptors induces conformational changes in the intracellular part. JAK1, JAK2, and TYK2 (Janus kinase) will be activated by IFN binding. In response to this activation, signal transducer and activator of transcription (STAT) proteins are recruited, which are then phosphorylated by JAKs; IFN-stimulated gene factor 3 (ISGF3) is formed and combined with IRF9 to form a complex. After translocation to the nucleus, the complex regulates ISG expression [21–29].

Although there are more studies on type III interferon, there are relatively few studies on animal interferon. In this study, porcine type III interferons (pIFNLs) were prepared using the baculovirus expression system. Using porcine type I interferons (pIFN α) as a positive control, the antiviral activities of pIFNLs were analyzed. The results showed that pIFNLs could not only activate a group of IFN-regulated genes but also significantly inhibit the replication of VSV-EGFP and PEDV in cells. pIFNL3 had the highest antiviral activity, followed by pIFNL1, and the antiviral activity of pIFN α was the lowest. In conclusion, we demonstrated that pIFNLs and pIFN α displayed robust antiviral activity against VSV-EGFP and PEDV infection. Moreover, pIFNLs preferably provide critical antiviral defenses compared to pIFN α .

2. Results

2.1. Preliminary Analysis of the Antiviral Activities of pIFNLs

To assess the antiviral activities of pIFNLs, the plasmid containing pIFNL1 and pIFNL3 were constructed based on pcDNA3.1 (Figure 1A). Transfecting human embryonic kidney cells (HEK293) with these constructs, the empty Vector and Mock served as negative controls. The WB result showed that pIFNL1 and pIFNL3 were expressed correctly, and a slightly smaller target band appeared in pIFNL1, which may have been caused by incomplete glycosylation (Figure 1B). Then the cell supernatant was collected after 48 h, and madin-Darby canine kidney (MDCK) cells seeded in 12-well plates (Corning, Corning, NY, USA) were treated for 12 h with serial dilutions of pIFNL preparations diluted 100-fold in DMEM. Cells were infected with VSV-EGFP at a multiplicity of infection (MOI) of 0.01. Fluorescence observation and flow cytometry were performed after 12 h. The results showed that pIFNL1 and pIFNL3 blocked VSV-EGFP infection significantly (Figure 1C,D). Furthermore, the proliferation of VSV-EGFP in MDCK cells was evaluated using the crystal violet staining assay (Figure 1E). The cell viability was significantly increased in the pIFNL-treated cells compared with the control groups. Moreover, with the increase of the dilution ratio, the virus infection ability became stronger, and the cell viability decreased obviously. The results show that pIFNL1 and pIFNL3 have antiviral activities and the inhibitory effect on the virus is dose-dependent.

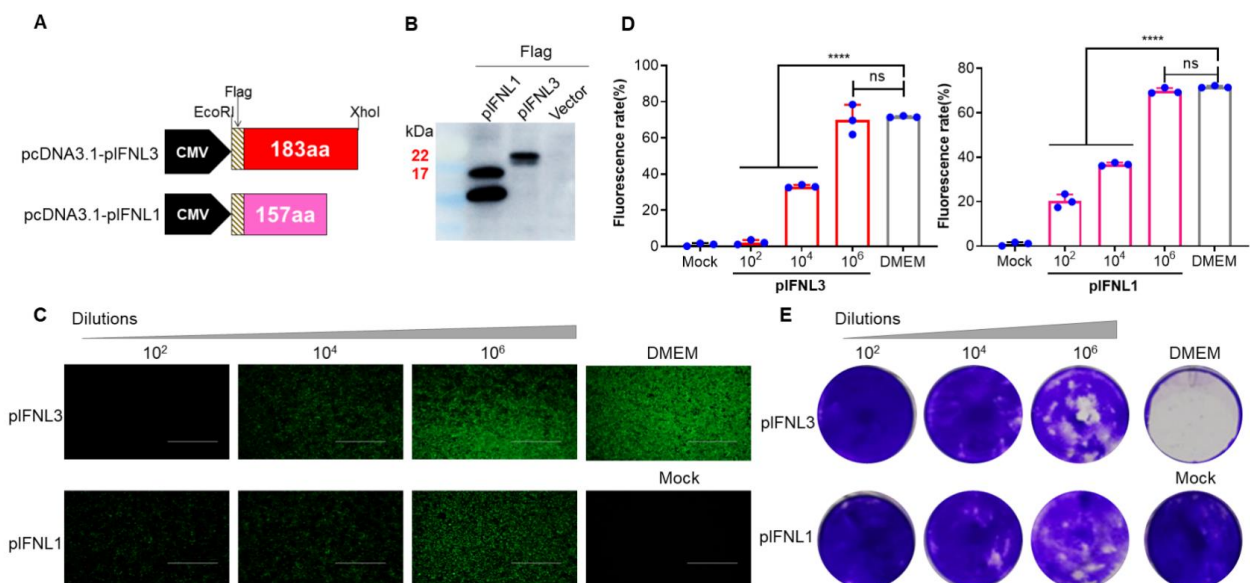


Figure 1. Preliminary analysis of antiviral activities of pIFNLs. (A) Schematics of the two recombinant plasmids pcDNA3.1-pIFNLs. (B) Expression of pIFNLs identified by WB. (C) The identified antiviral activities with different dilution times of IFNLs were analyzed by fluorescence observation using 12-well plates 12 h after VSV-EGFP (0.01 MOI) infection. The scale bar corresponds to 750 μ m. (D) The

identified antiviral activities with different dilution times of IFNLs were analyzed by flow cytometry using 12-well plates 12 h after VSV-EGFP (0.01 MOI) infection. ****, $p < 0.0001$; ns, no significant difference. (E) The identified antiviral activities with different dilution times of IFNLs were analyzed by crystal violet stain 36 h after VSV-EGFP (0.01 MOI) infection.

2.2. Generation of the Recombinant Baculoviruses *rBV-pIFNL1*, *rBV-pIFNL3*

To further evaluate the biological properties of pIFNLs, the baculovirus expression system (BES) was used to prepare the target protein. The pIFNL gene was optimized, synthesized, and subcloned into the PH promoter of the shuttle pFastBac™ 1 vector according to the protocols described previously [30]; pIFN α (gifted from XIANPUAIRUI SCIENCE, Gaomi, Shandong, China) served as a positive control (Figure 2A). The proteins were purified by ultracentrifugation with sucrose cushions. The SDS-PAGE assay and western blot showed that the target proteins were prepared successfully (Figure 2B,C). Then, the biological activities of pIFNLs and pIFN α were analyzed by a VSV-EGFP infection experiment according to the protocols (Figure 2D). The results of crystal violet staining showed that pIFNL1, pIFNL3, and pIFN α had biological activities (pIFNL1, 1.5×10^4 IU/0.1 mL; pIFNL3, 1.3×10^4 IU/0.1 mL; pIFN α , 1.28×10^3 IU/0.1 mL), and the antiviral effect was dose-dependent (Figure 2E).

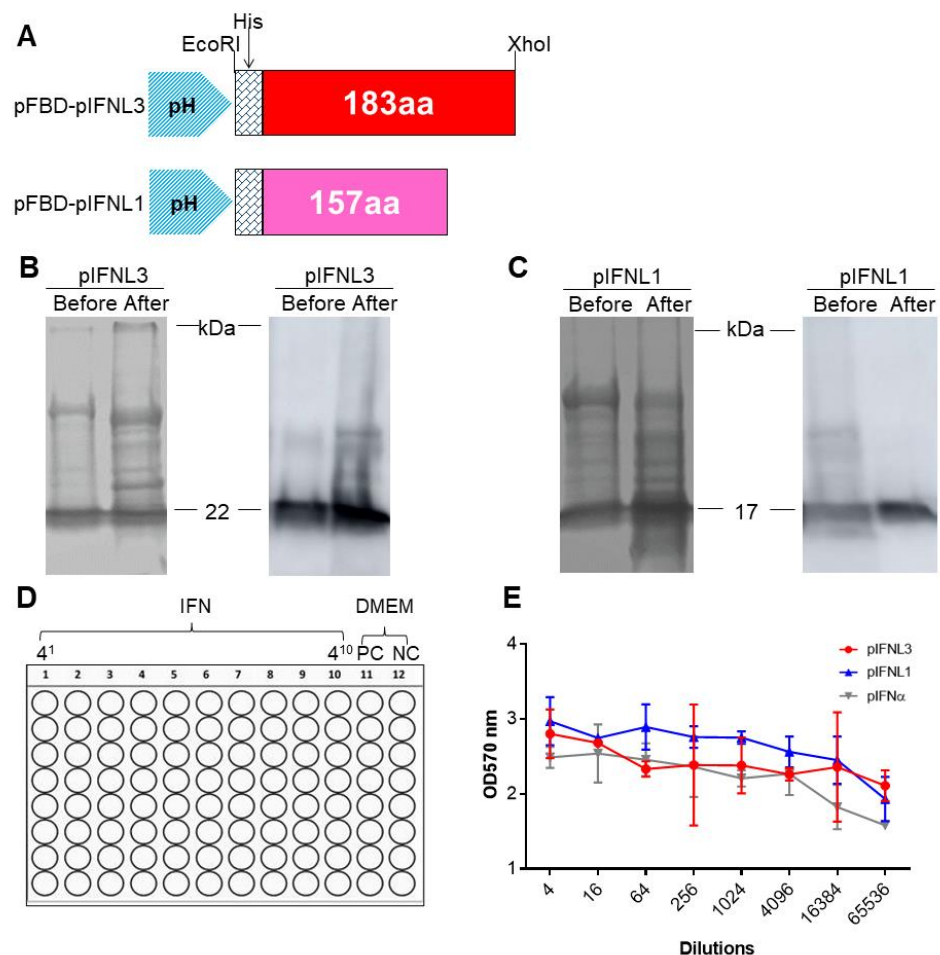


Figure 2. Expressions of pIFNLs by the baculovirus expression system and antiviral activity analysis, and pIFN α served as the control. (A) Schematics of the two recombinant shuttle plasmids pFBD-pIFNLs. (B,C) Expression of pIFNLs identified by SDS-PAGE and WB. “Before” means unpurified protein of pIFNLs. “After” means purified protein of pIFNLs. (D) The protocols for detecting the biological activity of pIFNLs. “PC” means positive control of the cells treated only with VSV-EGFP but not IFNs. (E) The OD570 nm value was used to evaluate the potency of interferon.

2.3. pIFNLs Inhibits VSV-EGFP Proliferation

To further determine whether IFNs had antiviral effects on other cells, both swine testis cells (ST) and african green monkey kidney cells (Vero) were treated with IFNs and infected with VSV-EGFP after 12 h to analyze the antiviral effects. The results showed that pIFNL1, pIFNL3, and pIFN α blocked the VSV-EGFP infection significantly (Figure 3A,B). Furthermore, the proliferation of VSV-EGFP in cells was evaluated using the crystal violet staining assay, and the cell viability in the interferon-treated group was higher than that in the control group (Figure 3C). Moreover, pIFNL3 had the highest antiviral activity, followed by pIFNL1; pIFN α had the worst effect.

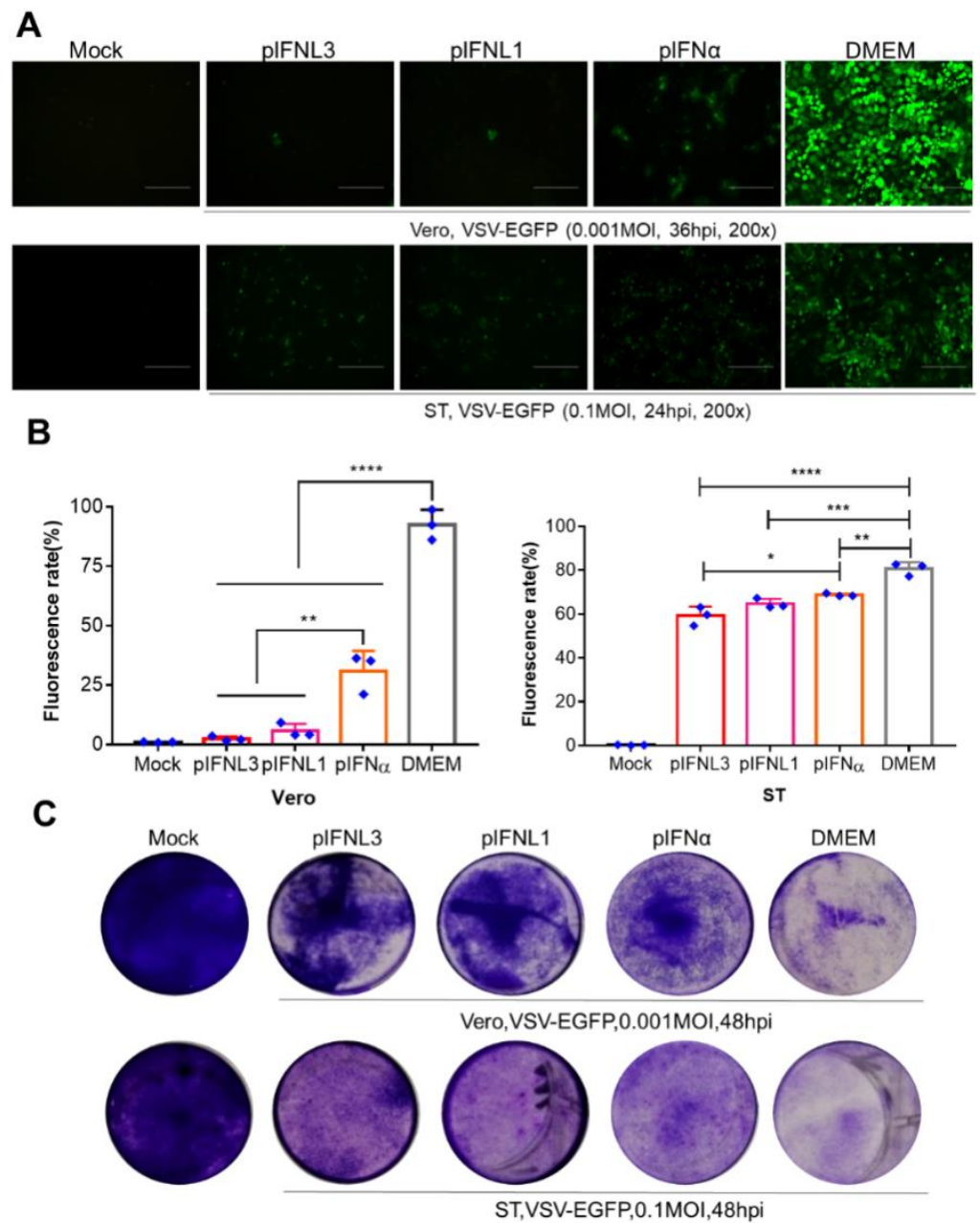


Figure 3. Antiviral activities of pIFNLs against VSV-EGFP in ST and Vero cells; pIFN α served as the control. (A) The identified antiviral activities of IFNLs were analyzed by crystal violet after VSV-EGFP infection. Mock means the normal cells without any treatment. The scale bar corresponds to 150 μ m. (B,C) Analysis of the antiviral activity of pIFNL1 by fluorescence observation and flow cytometry using 12-well plates after VSV-EGFP infection. *, $p < 0.05$; **, $p < 0.01$; ***, $p < 0.001$; ****, $p < 0.0001$.

2.4. pIFNLs Inhibits PEDV Proliferation in Vero Cells

To determine whether pIFNLs could inhibit PEDV proliferation, Vero cells were treated with pIFNLs (100 IU/mL) for 12 h followed by infection with PEDV at a multiplicity of infection (MOI) of 0.01; pIFN α was the positive control. IFA and WB were performed after 24 hpi to analyze the expression of the PEDV N protein (Figure 4A,B). The results showed that pIFNL1, pIFNL3, and pIFN α inhibited PEDV infection significantly. The proliferation of PEDV was evaluated using viral titers and qRT-PCR (Figure 4C,D); the results showed consistency with IFA and WB results. The above results show that both type I and type III interferons can inhibit the proliferation of PEDV on Vero cells, but there are differences in antiviral activities. Of the two type III interferons, pIFNL3 has higher antiviral activity.

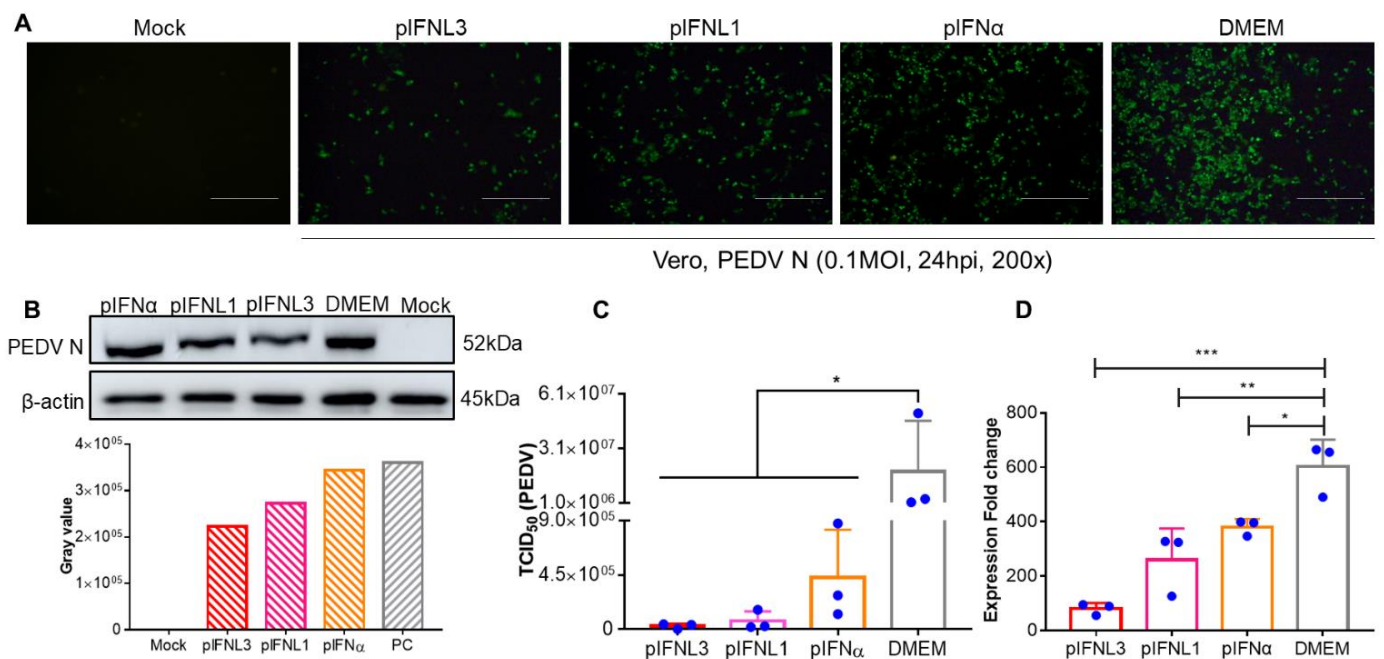


Figure 4. Antiviral activities of pIFNLs against PEDV in Vero; pIFN α served as the control. (A) Analysis of the antiviral activities of pIFNLs by IFA. The scale bar corresponds to 150 μ m. Using the PEDV N protein, specific antibodies as the primary antibodies, and FITC-labeled goat anti-rabbit IgG (H + L) as the secondary antibody, the virus protein was detected. (B) Analysis of antiviral activities of pIFNLs by WB. Using the PEDV N protein, specific antibodies as the primary antibodies, and HRP-labeled goat anti-rabbit IgG (H + L) as the secondary antibody, the virus protein was detected. (C) Analysis of the antiviral activities of pIFNLs by TCID₅₀. (D) Analysis of antiviral activities of pIFNLs by qPCR. *, $p < 0.05$; **, $p < 0.01$; ***, $p < 0.001$.

2.5. pIFNLs Induced ISGs Production

As we know, the receptor complex initiates the janus kinase (JAK)-signal transducer and activator of transcription (STAT) signaling pathways (JAK-STAT signal pathway) by binding to the common receptors and finally activates ISGF3. ISGF3 translocation leads to the transcriptional activation and massive expression of ISGs through the ISRE promoter to establish an antiviral state; IFNL exerts antiviral effects by inducing ISGs (Figure 5A). To demonstrate whether pIFNLs have similar mechanisms, we incubated pIFNLs with ST cells, which could stimulate ISG expression (Figure 5B). The results showed that pIFNLs upregulated the expressions of several antiviral proteins, including myxovirus resistant 1 (Mx1) and interferon-induced transmembrane (IFITM3).

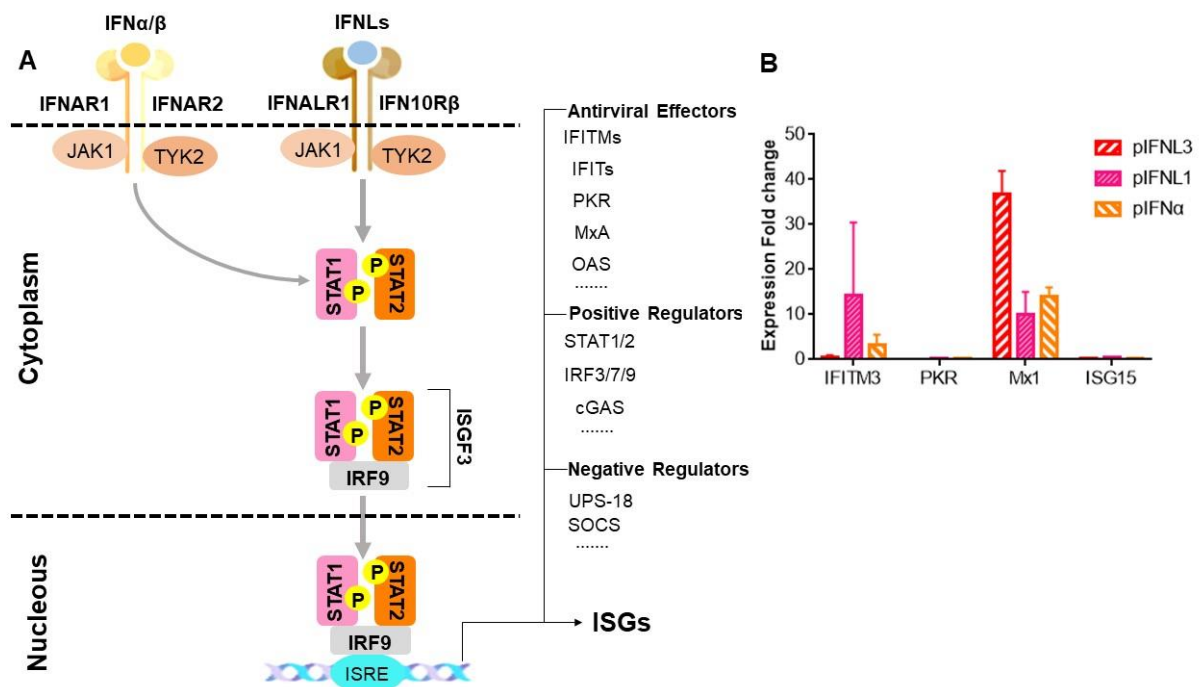


Figure 5. pIFNLs induced ISGS production. (A) Pattern diagram of ISG induction, induced by IFN. IFN interacts with the IFN receptor complex and initiates the formation of the ISGF3 transcription factor through the JAK-STAT pathway. The ISG induction, which determines the host's antiviral state, depends on the ISGF3 nuclear translocation and interaction with the ISRE promoter. (B) Transcriptional profiling of the IFITM3, double-stranded RNA-dependent protein kinase (PKR), Mx1, and interferon-stimulated gene 15 (ISG15) genes after the pIFNL-treated ST cells. The shown fold induction is the average performed in triplicate.

3. Discussion

In response to viral infection, interferons are among the most important molecules of innate immunity [31–33]. PEDV, an enteropathogenic alpha coronavirus, is responsible for swine diseases with high economic implications [34]. Acute malabsorption syndrome with watery diarrhea is caused by PEDV infection of the small intestinal epithelial cells in vivo, with symptoms of vomiting and anorexia in any age of a pig. Many viruses are shown to be inhibited by IFNL, both in vitro and in vivo. IFNL plays a pivotal role in inhibiting viral infections at mucosal surfaces [35]. Therefore, it is imperative that pIFNLs be analyzed for their role in anti-PEDV therapeutics, which are urgently needed. The purpose of this study was to examine the relative contribution of porcine IFNLs to controlling PEDV infection in vitro.

The antiviral activities of both subtypes of pIFNLs (pIFNL1 and pIFNL3) were experimentally demonstrated. Recombinant pIFNLs were prepared by the baculovirus expression system. Here, we report that both pIFNL1 and pIFNL3 have robust antiviral activity against PEDV and VSV-EGFP infections. Virus infection experiments showed that pIFNLs could inhibit PEDV and VSV infections in different cells in a dose-dependent manner. Our results on the comparison between pIFNLs and pIFN α against PEDV infection in Vero cells also demonstrate that pIFNLs more efficiently inhibit PEDV infection in Vero cells than pIFN α , although both inhibit PEDV infection. Moreover, pIFNL3 provided better viral inhibition against PEDV infection in Vero cells than pIFNL1. Transcriptional profiling of the antiviral proteins induced by pIFNLs was detected and showed that the expressions of these ISGs genes were upregulated after the treatment of pIFNLs, especially Mx1 and IFITM3. All of these imply that IFNL preferably provides critical antiviral defenses compared with type I IFN. Collectively, we demonstrated that pIFNLs and pIFN α displayed robust antiviral

activities against VSV-EGFP and PEDV infections. Moreover, our findings indicate that porcine IFNL might represent a promising therapeutic agent for PED in the future.

4. Materials and Methods

4.1. Cell Lines

Swine pulmonary alveolar macrophage (CRL2845), human embryonic kidney cells (HEK293), Madin–Darby canine kidney (MDCK), swine testis cells (ST), and African green monkey kidney cells (Vero) were cultured with Dulbecco’s Modified Eagle Medium (DMEM, HyClone, Logan, UT, USA), supplemented with 10% fetal bovine serum (FBS; Gibco, Grand Island, NY, USA), and 1% penicillin/streptomycin (Cytiva, Lewisville, TX, USA) at 37 °C with 5% CO₂. *Spodoptera frugiperda* (Sf9) cells (Invitrogen, Carlsbad, CA, USA) were cultured in SF-900™ II SFM medium (Gibco, Grand Island, NY, USA) supplemented with 10% FBS and incubated at 27 °C.

4.2. Viruses

A strain of the Vesicular stomatitis virus that contains an enhanced green fluorescent protein gene (VSV-EGFP) was kindly provided by Prof. ZhiGao Bu from the Haerbin Veterinary Research Institute, China [36]. The porcine epidemic diarrhea virus (PEDV) strain (GenBank no. OM814174) was previously isolated in our laboratory [37].

4.3. Plasmid Construction and Transfection

Using specific primers, reverse transcription polymerase chain reaction (RT-PCR) was used to generate cDNA for *pIFNL1* (GenBank no. FJ455508.1) and *pIFNL3* (GenBank no. GQ996936.1) (Table 1). Both genes were subcloned into eukaryotic expression vector pcDNA3.1 (Invitrogen, Carlsbad, CA, USA) with the FLAG-tag at their N-terminal. Target genes were verified through DNA sequencing (Comate Bioscience Co., Ltd., Changchun, Jilin, China). HEK293 cells were transfected with plasmids. At 48 h, cells and medium supernatant were harvested. Cells were lysed using 1× radioimmunoprecipitation assay (RIPA) buffer (Merck Millipore, Temecula, CA, USA) and supplemented with phenylmethanesulfonyl fluoride (PMSF, Beyotime, Shanghai, China).

Table 1. Primers in this study.

Class	Primer	Sequence (5'-3')	Length (bp)	Gene Name
PCR	pIFNL1F	GCTAGCGCCACCATGGATTACAAGGATGAC-	576	<i>pIFNL1</i>
	pIFNL1R	GACGATAAGATGGTATGCTACGGGGTCAC		
	pIFNL3F	AAGCTTCTAAGTGAATCCTCGCGC		
	pIFNL3R	GCTAGCGCCACCATGGATTACAAGGATGAC-		
qRT-PCR	PKRR	GACGATAAGATGGTATGCTACGGGGTCAC	90	<i>pPKR</i>
	PKRF	AAGCTTTCACTGTGCTGGGGACTG		
	Mx1F	TTGCGAGAAGGTAGAGCGTG	99	<i>pMx1</i>
	Mx1R	TCATCCCATCCCAGCAACC		
	IFITM3F	CAGAGGCAGCGGAATTGTGA	336	<i>pIFITM3</i>
	IFITM3R	TCCCGGTAAGTACTGACTTTGCC		
	ISG15F	CATGGAGGACCCCCAACATA	235	<i>pISG15</i>
	ISG15R	GCAAACGATGATGAACGCAA		
	β-actin F	TCCTGTTGATGGTGCAAAGC	160	<i>pβ-actin</i>
	β-actin R	ATACACGGTGCACATAGGCT		
		CTCCTGGGTAGGTGTCCG		
		CGTCGCACTTCATGATCGAG		

4.4. Analysis of Antiviral Activity of Interferon in Supernatant

Briefly, cells seeded in 12-well plates (Corning, Corning, NY, USA) were treated for 12 h with serial dilutions of supernatant preparation in 100-fold dilution in DMEM. Subsequently, cells were infected with VSV-EGFP. When obvious lesions appeared in the positive control hole, analysis of the antiviral activity by fluorescence observation, flow cytometry, and crystal violet took place.

4.5. Fluorescence Observation

After virus inoculation, fluorescence observation was carried out every 12 h with a Thermo Fisher Scientific EVOS M5000 microscope (Waltham, MA, USA).

4.6. Flow Cytometry (FCM)

At specified time points, EGFP-positive cells were collected, suspended with PBS, visualized by fluorescence microscopy, and quantified by the CytoFLEX flow cytometer (Beckman Coulter, Brea, CA, USA).

4.7. Crystal Violet Staining

After washing three times with PBS, the cells were stained with 0.1% crystal violet for 15 min at room temperature. To take macrographic images—stained cells were washed with PBS and air-dried.

4.8. Construction of the Recombinant Baculovirus and Preparation of Protein

The pFastBac™ 1 vector (Invitrogen, Carlsbad, CA, USA) was used to transfer the target gene into the baculovirus at the PH gene site. Both genes were codon-optimized according to amino acid sequences (Genscript, Nanjing, China) and synthesized. The resulting shuttle plasmids were named pFBD-pIFNL1 and pFBD-pIFNL3, respectively. The plasmids were transformed into competent DH10Bac™ *E. coli* cells (Biomed, Beijing, China), the recombinant bacmids rBD-pIFNL1 and rBD-pIFNL3 were identified by PCR (Table 1). Then, the recombinant baculovirus was rescued according to the literature [37], and the resulting recombinant baculoviruses were designated as rBV-pIFNL1 and rBV-pIFNL3, respectively. We blind-passaged the baculoviruses into Sf9 cells and kept them at $-80\text{ }^{\circ}\text{C}$. We examined the viral titer in the third passage using the manufacturer's instructions (Clontech, San Francisco, CA, USA). To prepare the protein, Sf9 cells in a shake flask (3×10^6 cells/well) were infected with the third passage rBVs (multiplicity of infection, MOI = 1) for 72 h. The medium supernatant was collected and ultracentrifuged through a 20% sucrose cushion at $216,428 \times g$, $4\text{ }^{\circ}\text{C}$ for 2 h. The pellets were suspended in PBS and evaluated using western blot.

4.9. Western Blot (WB)

Cells were collected and lysed and protein concentrations were determined using a bicinchoninic acid (BCA) protein assay kit (Beyotime, Shanghai, China). Proteins were mixed with a loading buffer and denatured by boiling. Total cell extracts were prepared and separated via 10% SDA-PAGE. The proteins were transferred onto the PVDF membrane (GE Healthcare, Chicago, IL, USA) and blocked with 5% skim milk. Using specific antibodies as the primary antibodies and HRP labeled goat anti-mouse/rabbit IgG (H + L) as the secondary antibody, the protein was detected. The protein band was developed using GEGEGNOME XRQ.

4.10. Assay of Recombinant Interferon Titer

MDCK cells seeded in 96-well plates (Corning, Corning, NY, USA) were treated for 12 h with serial dilutions of pIFNL preparations diluted four-fold in DMEM. Subsequently, cells were infected with VSV-EGFP (the final concentration was 100 TCID₅₀). When obvious lesions appeared in the positive control hole, the crystal violet staining assay was used to evaluate the interferon titer, and calculated by the Reed–Muench method.

4.11. Virus Infection

Cells were treated with pIFNs (100 IU/mL) for 12 h followed by infection with indicated viruses at suitable MOIs (MDCK, VSV-EGFP, 0.005 MOI; Vero, VSV-EGFP, 0.001 MOI; ST, VSV-EGFP, 0.1 MOI; Vero, PEDV, 0.1 MOI, respectively), and the DMEM served as the negative control.

4.12. Indirect Immunofluorescence (IFA)

Vero cells were seeded into 12-well plates at a density of 5×10^5 cells/well and incubated by pIFNLs for 12 h. Then, cells were infected with PEDV at an MOI of 0.01 and cultured for a further 24 h. The cells were then fixed with ice-cold 4% paraformaldehyde (Beyotime, Shanghai, China) for 1 h and washed three times with PBS. Next, cells were blocked with 0.1% Triton X-100 (Beyotime, Shanghai, China) and 5% skim milk for 1 h. After washing a further three times with PBS, FITC-conjugated PEDV N protein-specific primary antibodies (Medgene Labs, Brookings, SD, USA) were added and incubated for 2 h at 37 °C. Cells were then washed; images were captured using a Thermo Fisher Scientific EVOS M5000 microscope.

4.13. TCID₅₀

Vero cells were seeded into 96-well plates at 1×10^5 cells per well, continuously diluting the sample 10-fold, 100 μ L/well (three repetitions for each sample). After the cells had obvious CPE, the number of CPE holes under each dilution was recorded, and TCID₅₀ was calculated by the Reed–Muench method.

4.14. qRT-PCR

Total RNA was extracted from cells (Sangon Biotech, Shanghai, China) according to the manufacturer's instructions. cDNA was analyzed using the Fast Start Universal SYBR Green Master Mix (Roche, San Francisco, CA, USA) for quantitative PCR (qPCR). The primer sequences are listed in Table 1. Relative quantities were calculated and normalized to β -actin using the $2^{-\Delta\Delta CT}$ method.

4.15. Statistical Analyses

With the one-way analysis of variance (ANOVA; two-tailed, confidence intervals (CI) 95%), the statistical analysis was conducted using GraphPad 8.0 (GraphPad Software, San Diego, CA, USA), as indicated by the *p*-value. The results were statistically significant at *p* < 0.05. For each separate set of assays, at least three independent experiments were evaluated. The results are expressed as the mean \pm standard deviation (SD).

5. Conclusions

In conclusion, the baculovirus system was used to construct and express pIFNLs; pIFNLs not only could inhibit PEDV but also VSV infection in different cells in a dose-dependent manner. The expressions of ISGs genes were upregulated after the treatment of pIFNLs, especially Mx1 and IFITM3.

Author Contributions: Conceptualization, C.L. and N.J.; methodology, J.C.; validation, P.L., W.Z. and L.S.; formal analysis, P.H., Z.G. and Y.J.; writing—original draft preparation, J.C.; writing—review and editing, C.L.; visualization, W.X. and P.L.; supervision, C.L. and N.J.; project administration, C.L. and N.J.; funding acquisition, C.L. and N.J. All authors have read and agreed to the published version of the manuscript.

Funding: This work was supported by the National Key Research and Development Program of China (no. 2021YFD1801103-6); the National Natural Science Foundation of China (no. 31972719); CAMS Innovation Fund for Medical Sciences (2020-12M-5-001). The funders had no role in the study design, data collection and analysis, decision to publish, or preparation of the manuscript.

Institutional Review Board Statement: Not applicable.

Informed Consent Statement: Not applicable.

Data Availability Statement: All data generated or analyzed during this study are included in this published article.

Conflicts of Interest: The authors declare no conflict of interest.

References

1. LaFleur, D.W.; Nardelli, B.; Tsareva, T. Interferon- κ , a Novel Type I Interferon Expressed in Human Keratinocytes. *J. Biol. Chem.* **2001**, *276*, 39765–39771. [[CrossRef](#)] [[PubMed](#)]
2. Takaoka, A.; Yanai, H. Interferon signalling network in innate defence. *Cell. Microbiol.* **2006**, *8*, 907–922. [[CrossRef](#)] [[PubMed](#)]
3. Isaacs, A.; Lindenmann, J. Virus interference. I. The interferon. *Proc. R. Soc. Lond. Ser. B Biol. Sci.* **1957**, *147*, 258–267. [[CrossRef](#)]
4. Kotenko, S.V.; Gallagher, G.; Baurin, V.V. IFN-lambda mediates antiviral protection through a distinct class II cytokine receptor complex. *Nat. Immunol.* **2003**, *4*, 69. [[CrossRef](#)]
5. Sheppard, P.; Kindsvogel, W.; Xu, W. IL-28, IL-29 and their class II cytokine receptor IL-28R. *Nat. Immunol.* **2003**, *4*, 63–68. [[CrossRef](#)]
6. Pestka, S.; Krause, C.D.; Sarkar, D.; Walter, M.R.; Shi, Y.; Fisher, P.B. Interleukin-10 and related cytokines and receptors. *Annu. Rev. Immunol.* **2004**, *22*, 929–979. [[CrossRef](#)]
7. Ank, N.; West, H.; Bartholdy, C.; Eriksson, K.; Thomsen, A.R.; Paludan, S.R. Lambda Interferon (IFN- λ), a Type III IFN, Is Induced by Viruses and IFNs and Displays Potent Antiviral Activity against Select Virus Infections In Vivo. *J. Virol.* **2006**, *80*, 4501–4509. [[CrossRef](#)]
8. Ank, N.; Iversen, M.B.; Bartholdy, C. An Important Role for Type III Interferon (IFN- λ /IL-28) in TLR-Induced Antiviral Activity. *J. Immunol.* **2008**, *180*, 2474. [[CrossRef](#)]
9. Sommereyns, C.; Paul, S.; Staeheli, P.; Michiels, T. IFN-lambda (IFN- λ) is expressed in a tissue-dependent fashion and primarily acts on epithelial cells in vivo. *PLoS Pathog.* **2008**, *4*, e1000017. [[CrossRef](#)]
10. Mordstein, M.; Kochs, G.; Dumoutier, L.; Renaud, J.C.; Paludan, S.R.; Klucher, K.; Staeheli, P. Interferon- λ contributes to innate immunity of mice against influenza A virus but not against hepatotropic viruses. *PLoS Pathog.* **2008**, *4*, e1000151. [[CrossRef](#)]
11. Mordstein, M.; Neugebauer, E.; Ditt, V.; Jessen, B.; Rieger, T.; Falcone, V.; Sorgeloos, F.; Ehl, S.; Mayer, D.; Kochs, G. Lambda interferon renders epithelial cells of the respiratory and gastrointestinal tracts resistant to viral infections. *J. Virol.* **2010**, *84*, 5670–5677. [[CrossRef](#)] [[PubMed](#)]
12. Pulverer, J.E.; Rand, U.; Lienenklaus, S. Temporal and Spatial Resolution of Type I and III Interferon Responses In Vivo. *J. Virol.* **2010**, *84*, 8626–8638. [[CrossRef](#)]
13. Pott, J.; Mahlaköiv, T.; Mordstein, M. IFN-lambda determines the intestinal epithelial antiviral host defense. *Proc. Natl. Acad. Sci. USA* **2011**, *108*, 7944. [[CrossRef](#)] [[PubMed](#)]
14. Mahlaköiv, T.; Hernandez, P.; Gronke, K.; Diefenbach, A.; Staeheli, P. Leukocyte-Derived IFN- α/β and Epithelial IFN- λ Constitute a Compartmentalized Mucosal Defense System that Restricts Enteric Virus Infections. *PLoS Pathog.* **2015**, *11*, e1004782. [[CrossRef](#)] [[PubMed](#)]
15. Hernández, P.P.; Mahlaköiv, T.; Yang, I. Interferon- λ and interleukin 22 act synergistically for the induction of interferon-stimulated genes and control of rotavirus infection. *Nat. Immunol.* **2015**, *16*, 698–707. [[CrossRef](#)]
16. Lin, J.D.; Feng, N.; Sen, A. Distinct Roles of Type I and Type III Interferons in Intestinal Immunity to Homologous and Heterologous Rotavirus Infections. *PLoS Pathog.* **2016**, *12*, e1005600. [[CrossRef](#)]
17. Saxena, K.; Simon, L.M.; Zeng, X.-L. A paradox of transcriptional and functional innate interferon responses of human intestinal enteroids to enteric virus infection. *Proc. Natl. Acad. Sci. USA* **2017**, *114*, E570–E579. [[CrossRef](#)]
18. Galani, I.E.; Triantafyllia, V.; Eleminiadou, E.E. Interferon- λ Mediates Non-redundant Front-Line Antiviral Protection against Influenza Virus Infection without Compromising Host Fitness. *Immunity* **2017**, *46*, 875–890.e6. [[CrossRef](#)]
19. Pervolaraki, K.; Stanifer, M.L.; Münchau, S. Type I and type III interferons display different dependency on mitogen-activated protein kinases to mount an antiviral state in the human gut. *Front. Immunol.* **2017**, *8*, 459. [[CrossRef](#)]
20. Pervolaraki, K.; Rastgou Talemi, S.; Albrecht, D. Differential induction of interferon stimulated genes between type I and type III interferons is independent of interferon receptor abundance. *PLoS Pathog.* **2018**, *14*, e1007420. [[CrossRef](#)]
21. Lavoie, T.B.; Kalie, E.; Crisafulli-Cabatu, S. Cytokine Binding and activity of all human alpha interferon subtypes. *Cytokine* **2011**, *56*, 282–289. [[CrossRef](#)] [[PubMed](#)]
22. Jaks, E.; Gavutis, M.; Uzé, G.; Martal, J.; Piehler, J. Differential Receptor Subunit Affinities of Type I Interferons Govern Differential Signal Activation. *J. Mol. Biol.* **2007**, *366*, 525–539. [[CrossRef](#)] [[PubMed](#)]
23. Jaitin, D.A.; Roisman, L.C.; Jaks, E. Inquiring into the Differential Action of Interferons (IFNs): An IFN-2 Mutant with Enhanced Affinity to IFNAR1 Is Functionally Similar to IFN-beta. *Mol. Cell. Biol.* **2006**, *26*, 1888–1897. [[CrossRef](#)] [[PubMed](#)]
24. François-Newton, V.; de Freitas Almeida, G.M.; Payelle-Brogard, B. USP18-based negative feedback control is induced by type I and type III interferons and specifically inactivates interferon α response. *PLoS ONE* **2011**, *6*, e22200. [[CrossRef](#)]
25. Bazan, J.F. Structural design and molecular evolution of a cytokine receptor superfamily. *Proc. Natl. Acad. Sci. USA* **1990**, *87*, 6934–6938. [[CrossRef](#)]
26. Renaud, J.C. Class II cytokine receptors and their ligands: Key antiviral and inflammatory modulators. *Nat. Rev. Immunol.* **2003**, *3*, 667–676. [[CrossRef](#)]
27. Cohen, B.; Novick, D.; Barak, S. Ligand-Induced Association of the Type I Interferon Receptor Components. *Mol. Cell. Biol.* **1995**, *15*, 4208–4214. [[CrossRef](#)]
28. Piehler, J.; Schreiber, G. Mutational and structural analysis of the binding interface between type I interferons and their receptor ifnar₂. *J. Mol. Biol.* **1999**, *294*, 223–237. [[CrossRef](#)]

29. Lamken, P.; Lata, S.; Gavutis, M.; Piehler, J.; Wolfgang, J. Ligand-induced Assembling of the Type I Interferon Receptor on Supported Lipid Bilayers. *J. Mol. Biol.* **2004**, *341*, 303–318. [[CrossRef](#)]
30. Xu, W.; Du, S.; Li, T.; Wu, S.; Jin, N.; Ren, L.; Li, C. Generation and Evaluation of Recombinant Baculovirus Coexpressing GP5 and M Proteins of Porcine Reproductive and Respiratory Syndrome Virus Type 1. *Viral Immunol.* **2021**, *34*, 697–707. [[CrossRef](#)]
31. Zhou, J.-H.; Wang, Y.-N.; Chang, Q.-Y.; Ma, P.; Hu, Y.-H.; Cao, X. Type III Interferons in Viral Infection and Antiviral Immunity. *Cell. Physiol. Biochem.* **2018**, *51*, 173. [[CrossRef](#)] [[PubMed](#)]
32. Kim, Y.-M.; Shin, E.-C. Type I and III interferon responses in SARS-CoV-2 infection. *Exp. Mol. Med.* **2021**, *53*, 750. [[CrossRef](#)] [[PubMed](#)]
33. Stanifer, M.L.; Pervolaraki, K.; Boulant, S. Differential Regulation of Type I and Type III Interferon Signaling. *J. Mol. Sci.* **2019**, *20*, 1445. [[CrossRef](#)]
34. Jung, K.; Saif, L.J.; Wang, Q. Porcine epidemic diarrhea virus (PEDV): An update on etiology, transmission, pathogenesis, and prevention and control. *Virus Res.* **2020**, *286*, 198045. [[CrossRef](#)]
35. Baldrige, M.T.; Nice, T.J.; McCune, B.T.; Yokoyama, C.C.; Kambal, A.; Wheadon, M.; Diamond, M.S.; Ivanova, Y.; Artyomov, M.; Virgin, H.W. Commensal microbes and interferon-lambda determine persistence of enteric murine norovirus infection. *Science* **2015**, *347*, 266–269. [[CrossRef](#)] [[PubMed](#)]
36. Chen, W.; Wen, Z.; Zhang, J.; Li, C.; Huang, K.; Bu, Z. Establishing a safe, rapid, convenient and low-cost antiviral assay of interferon bioactivity based on recombinant VSV expressing GFP. *J. Virol. Methods* **2018**, *252*, 1–7. [[CrossRef](#)] [[PubMed](#)]
37. Song, L.; Chen, J.; Hao, P. Differential Transcriptomics Analysis of IPEC-J2 Cells Single or Coinfected with Porcine Epidemic Diarrhea Virus and Transmissible Gastroenteritis Virus. *Front Immunol.* **2022**, *25*, 13. [[CrossRef](#)]